Inelastic and quasielastic collisions of Rydberg atoms with the heavy rare-gas atoms

Vladimir S. Lebedev* and Ilya I. Fabrikant
Department of Physics and Astronomy, University of Nebraska, Lincoln, Nebraska 68588-0111

(Received 5 March 1996)

A theory of inelastic n,l-changing and quasielastic l-mixing collisions of Rydberg atoms with the heavy rare-gas atoms is developed. It is based on the semiclassical impact-parameter approach combined with the normalized perturbation theory. Semiclassical formulas for scaled transition probabilities and cross sections as functions of the inelasticity parameter and the collision strength are analyzed. This approach gives a general description of collisional $nl \rightarrow n'$ transitions independently of the specific values of the principal quantum number, the relative velocity, and the type of colliding atoms. The energy and angular dependence of the electron-atom scattering amplitude is included in the theory by incorporating the impulse-approximation results in the weak-coupling limit. The Ramsauer-Townsend effect affects significantly the values of the cross sections, especially for the inelastic transitions with large energy transfer. The results obtained are used in calculations of the quenching cross sections for the Rb(nS,nD,nF) atoms in collisions with Ar, Kr, and Xe. Comparison of theory and experiment is made in a wide range of the principal quantum numbers and transition energy defects. [S1050-2947(96)02509-7]

PACS number(s): 34.60.+z

I. INTRODUCTION

Collisions of highly excited (Rydberg) atoms with neutral particles is being intensively studied both experimentally and theoretically (see [1–3] and references therein). A detailed analysis of the main theoretical approaches to collisions involving highly excited atoms and their applications to various processes has been the subject of several review articles [1a–c,3]. In spite of significant progress in the physics of the Rydberg-atom–neutral-particle collisions made during the last two decades, many important problems in this field remain unsolved and require further detailed investigations. There is no general theoretical approach describing different types of processes in a wide range of the principal quantum numbers and transition energy defects. At the same time, the behavior of transition probabilities and cross sections of Rydberg-atom–neutral-particle collisions depends drastically both on the principal quantum number n and the energy defect of the process, as well as on a particular type of colliding particles and their relative velocity. In particular, the cross sections and rate constants turn out to be quite different for transitions with small and large energy transferred to the highly excited electron from the relative motion of neutral projectile and ionic core of the Rydberg atom.

There are few efficient theoretical approaches to collisions of Rydberg atoms with neutral particles. Most of them are based on the quantum impulse approximation [1b] and its semiclassical version [1c] (binary-encounter theory in the momentum representation), the Born approximation with the Fermi pseudopotential [1a], and on the semiclassical impact-parameter method [1a,1b]. The latter is widely used in combination with the first-order time-dependent perturbation theory. However, the approaches based on perturbation theory are valid in the range of weak coupling of Rydberg states. Therefore, for collisions with small energy transfer, they can be applied to calculations of the cross sections only at high principal quantum numbers.

On the other hand, the application of the close-coupling method to collisions involving Rydberg atoms becomes very difficult at high principal quantum numbers due to the presence of a great number of closely spaced levels. Simple versions of this method at low $n(<10)$ were used for the quasielastic l-mixing process in thermal Rydberg-atom–rare-gas-atom collisions [1a]. Semiclassical calculations [4] of the n-changing process in thermal Na(ns)+He collisions were performed by the close-coupling method at $n=6$ and 9. The same approach was used [5] for the description of l mixing in rotationally elastic collisions of Rydberg atoms with strongly polar molecules HF and HCl in a wide range of n. However, reliable semiclassical calculations based on numerical integration of the close-coupling equations for the transition amplitudes were carried out only for few specific processes involving Rydberg atoms.

Furthermore, numerical calculations have not yet given a general picture for different processes with regard to their dependence on the quantum numbers of the Rydberg atom, the relative velocity V of colliding particles, and the transition energy defect $|\Delta E_{fi}|$. An analytical or a semianalytical description of Rydberg-atom–neutral-particle collisions is desirable for understanding the cross section dependencies on the main physical parameters.

Here we consider in detail inelastic n,l-changing and quasielastic l-mixing processes in collisions of Rydberg atoms with neutral atomic targets induced by the electron–perturber interaction. Collisional processes accompanied by small and large energy transfer were usually studied independently from each other. It is due to a significant difference in the typical magnitudes of the cross sections for quasielastic l-mixing and inelastic n,l-changing processes at thermal energies. Many theoretical models have been used for the l-mixing processes in collisions of the Rydberg atoms with the ground-state rare-gas atoms (see reviews [1,3] and refer-

*Permanent address: P.N. Lebedev Physical Institute, Leninsky Prosp. 53, Moscow 117924, Russia.

ences therein). Some recent calculations employed a pure classical model [6], the free-electron model [7], and the eikonal approximation [8]. Several calculations were also performed for the inelastic n,l-changing processes [3].

Recently a semiclassical approach combined with the normalized perturbation theory was proposed [9]. It gives a general description of n,l-changing and l-mixing processes in a wide range of the principal and orbital quantum numbers and transition energy defects. The most part of calculations of probabilities, cross sections and rate constants for $nl \to n'$ transitions can be performed in the analytical form. A similar analytical approach was previously used [10] for description of elastic scattering and inelastic transitions between the fine-structure components of Rydberg atom induced by collisions with neutral particles.

In the present paper we elaborate this approach and apply it to thermal inelastic and quasielastic collisions of Rydberg atoms with the heavy rare-gas atoms Ar, Kr, and Xe in the ground states. In Sec. II A we outline the main idea of the theoretical approach and present the basic equations.

In Sec. II B we analyze the role of the angular and energy dependence of the amplitude for scattering of Rydberg electrons by heavy rare-gas atoms. A substantial part of the previous calculations of Rydberg-atom–rare-gas-atom collisions was performed using the scattering-length approximation for the amplitude $f_{eB} = -L$ of elastic electron-atom scattering. To improve the results of calculations for the l-mixing and n,l-changing processes induced by the heavy rare-gas atoms Hickman [11,12] used the parameter $[\sigma_{\rm el}(\epsilon_n)/4\pi]^{1/2}$ instead of the standard scattering length L. Here $\sigma_{\rm el}(\epsilon_n)$ is the total elastic free-electron scattering cross section for the mean kinetic energy ϵ_n of the orbital electron motion. The semiclassical model of de Prunelé and Pascale [13] for quasielastic collisions takes into account the actual energy dependence of the free-electron scattering cross section and averages it over the momentum distribution.

Another approach takes into account the low-energy behavior of the scattering amplitude as a function of the momentum transfer Q in the Born-type form $f_{eB} = -L - \pi\alpha Q/4$ [14,15], where α is the atomic polarizability. These calculations [16–18] were performed in the impulse approximation for the quasielastic state-changing process at high principal quantum numbers n. In these calculations the second term of the low-energy expansion is important but it does not affect drastically the values of the cross sections.

To describe the quasielastic and inelastic transitions in a wide range of n and energy defects it is necessary to take into account the actual behavior of the amplitude for elastic electron heavy-rare-gas atom scattering not only at very low energies but also in the region $\epsilon \sim 0.2-1$ eV. In this region, the dependence of the scattering amplitude for Ar, Kr, and Xe atoms on the scattering angle θ and electron momenta k cannot be reduced to one parameter Q. In Sec. II B we present a method allowing inclusion of the actual k and θ dependencies for the amplitude f_{eB}.

In Sec. II C we give a detailed analysis of the probabilities and cross sections as functions of the main physical parameters: the inelasticity parameter, the collision strength, and the scaled impact parameter. We show that the transition probability and the ratio of the cross section to the geometrical area of the Rydberg atom, expressed in terms of the identified parameters, do not include explicitly the dependencies on the principal quantum number n, relative velocity V, and the effective scattering length L. Thus, calculations and analysis of these dependencies can provide general data for inelastic and quasielastic $nl \to n'$ transitions in Rydberg-atom–neutral-particle collisions independently of a particular type of colliding partners. We will also analyze the range of impact parameters and the Rydberg-electron–ion-core separations which make the main contribution to the transition probability and the cross section.

It should be noted that an approximate scaling formula for the quasielastic l-mixing cross section was previously proposed by Hickman [11] by fitting the numerical results of close-coupling [19] and Born calculations in the momentum representation [12]. It was widely used for a rapid estimation of the l-mixing cross sections in the Rydberg-atom–neutral-particle collisions. It can be considered as the first step toward the description of the Rydberg-atom–neutral-particle collisions in terms of the scaled parameters characterizing the efficiency of collision and the transition energy defect. However, the range of its validity is restricted by small values of the energy defect and it becomes inapplicable for the inelastic $nl \to n'$ transitions with a large energy transfer.

In Sec. III we present calculations of the inelastic n,l-changing and quasielastic l-mixing processes in thermal collisions of Rydberg Rb atoms with the ground-state Ar, Kr, and Xe atoms. They have been performed in a wide range of the principal quantum numbers $(8 < n < 80)$ for various Rydberg nl states (nS, nD, nF) having quite different values of the quantum defects δ_l. Comparison with available experimental data will be also given. Atomic units $e = m = \hbar = 1$ are used throughout the paper.

II. THEORY

A. Basic equations of the normalized perturbation theory and semiclassical approach to the $nl \to n'$ collisional transitions

The general formulation of the normalized perturbation theory [20,21] involves the K-matrix method. Direct application of this method to collisions involving highly excited atoms becomes difficult due to the presence of a great number of closely spaced levels. A simple modification of the normalized Born approximation was widely used for a description of transitions between Rydberg states in collisions with charged particles [3]. An analytical approach based on the semiclassical method and the normalized perturbation theory was proposed in Ref. [9] for description of the $nl \to n'$ transitions in Rydberg-atom–neutral-particle collisions. A similar approach was used [10] for transitions between the fine-structure components and for elastic scattering.

Here we outline the main idea of the semiclassical approach [9] and present the basic equations needed for our analysis and calculations. Within the framework of the impact-parameter method, the relative motion of a Rydberg atom A and a neutral target B is considered to be rectilinear, so that $\mathbf{R}(t) = \boldsymbol{\rho} + \mathbf{V}t$, where $\mathbf{R}$ is the radius vector of the target B relative to the ion core A^+, and $\boldsymbol{\rho}$ is the impact-parameter vector. The idea of the semiclassical approach [9] is based on the separation of the whole range of the impact parameters into two regions ($0<\rho<\rho_0$) and ($\rho_0<\rho$) with qualitatively different behavior of the transition probability $W_{fi}(\rho)$. At large impact parameters $\rho>\rho_0$ the coupling between Rydberg states is weak, and the transition probability can be calculated using the general formula [22]

$$W_{fi}^{\rm pt}(\rho)=\left|\int_{-\infty}^{+\infty}V_{fi}[\mathbf{R}(t)]\exp(i\omega_{fi}t)dt\right|^2 \quad (1)$$

of the first-order time-dependent perturbation theory. Here $\omega_{fi}=|\Delta E_{fi}|$ is the transition frequency, $V_{fi}[\mathbf{R}(t)]=\langle\phi_f(\mathbf{r})|V[\mathbf{r},\mathbf{R}(t)]|\phi_i(\mathbf{r})\rangle$ is the matrix element of interaction between the Rydberg atom and the neutral target, $\mathbf{r}$ is the radius vector of the highly excited electron, and $\phi_i(\mathbf{r})$, $\phi_f(\mathbf{r})$ are the wave functions of the Rydberg atom in the initial and final states, respectively.

At small $\rho<\rho_0$, due to strong coupling between Rydberg states, the first-order perturbation theory leads to overestimated values of the probability of the $i\to f$ transition. In the simplest version of the normalized perturbation theory the transition probability in the region of strong coupling is equal to a constant c of the order of unity [23]. The magnitude of the impact parameter ρ_0, which separates the region of weak coupling ($\rho>\rho_0$) from that of strong coupling ($\rho<\rho_0$), is to be found from the equation

$$W_{fi}^{\rm pt}(\rho_0)=c. \quad (2)$$

For the cross section $\sigma_{fi}(V)$ of the $i\to f$ transition we obtain [9,10]

$$\sigma_{fi}=\pi\rho_0^2c+2\pi\int_{\rho_0}^{\infty}W_{fi}^{\rm pt}(\rho)\rho\, d\rho. \quad (3)$$

The choice of parameter c contains some ambiguities. According to Gersten [23] its value should be close to 1. On the other hand, as will be shown in Sec. II C, in the weak-coupling region the theoretical results are almost independent of c whereas in the strong-coupling limit Eq. (3) gives for the quasielastic cross section $4\pi c n_*^4$. According to Hickman's scaling formula, [11] the cross section in this limit should approach $0.6\pi n_*^4$ corresponding to $c=0.15$. Our choice is $c=0.25$. This value is based both on Hickman's scaling formula and on comparison of our results with the results of close-coupling calculations and experiments obtained in the strong-coupling region (see [1–3] and references therein). In further discussion we will not specify the value of c, but in all calculations we will be using $c=0.25$.

For the radial parts of the wave functions $\phi_i(\mathbf{r})$ and $\phi_f(\mathbf{r})$ of the Rydberg atom we use the JWKB approximation [22]

$$R_{n_*l}=\left(\frac{2}{\pi n_*^3}\right)^{1/2}\frac{\cos\Phi_r}{rk_r^{1/2}},\quad \Phi_r=\int_{r_1}^{r}k_r dr-\pi/4. \quad (4)$$

Here $n_*=n-\delta_l$ is the effective principal quantum number, k_r is the radial momentum of the highly excited electron in the Coulomb field of the ionic core

$$k_r=\left[-\frac{1}{n_*^2}+\frac{2}{r}-\frac{(l+1/2)^2}{r^2}\right]^{1/2},\quad r_{1,2}=n_*^2(1\pm e) \quad (5)$$

r_1,r_2 are the left and right turning points and $e=[1-(l+1/2)^2/n_*^2]^{1/2}$ is the eccentricity of the Rydberg-electron orbit. If we have to sum the probability of the $nl\to n'$ transition over a large number of degenerate states with different orbital quantum numbers l', we use the JWKB approximation for the angular parts $Y_{l'm'}(\theta,\phi)$ of the Rydberg-electron wave function [3].

We assume now that the interaction between the perturbing atom B and the ion core can be ignored, and the short-range interaction between the Rydberg electron and B can be described by the zero-range Fermi pseudopotential $V_{eB}(|\mathbf{r}-\mathbf{R}|)=2\pi L_{\rm eff}\delta(\mathbf{r}-\mathbf{R})$, where $L_{\rm eff}$ is the effective scattering length for electron-perturber scattering. In contrast to the standard scattering length L, $L_{\rm eff}$ depends on collision parameters and n. This dependence will be discussed in Sec. II B.

The final equation for the transition probability can be expressed in terms of the incomplete elliptic integrals of the first kind [9]

$$W_{n',nl}(\rho)=\begin{cases} c, & 0<\rho<\rho_0\\ \dfrac{L_{\rm eff}^2}{2\pi n_*^6V^2\sqrt{\rho}}\{F(\varphi_2,k)-F(\varphi_1,k)+2\Theta(\tilde{\rho}-\rho)F(\varphi_1,k)\}, & \rho_0<\rho<\rho_{\max}\\ 0, & \rho_{\max}<\rho. \end{cases} \quad (6)$$

Here $\Theta(z)=1$ for $z\geqslant0$ and $\Theta(z)=0$ for $z<0$; and

$$F(\varphi,k)=\int_0^{\varphi}(1-k^2\sin^2\theta)^{-1/2}d\theta,\quad k=[(1-\rho/2n_*^2)/2]^{1/2} \quad (7)$$

(see, for example, Ref. [24]), while the arguments φ_1 and φ_2 in Eq. (6) are

$$\varphi_s=\arcsin\left[\left(\frac{R_s(\rho)-\rho}{(1-\rho/2n_*^2)R_s(\rho)}\right)^{1/2}\right],\quad s=1,2. \quad (8)$$

Parameters $R_1(\rho)=2n_*^2x_1^{(\lambda)}(y)$ and $R_2(\rho)=2n_*^2x_2^{(\lambda)}(y)$, ($R_1\leqslant R_2$), are determined from the equation

$$y=\phi_\lambda(x),\quad \phi_\lambda(x)=(2\lambda)^{1/2}\frac{x^{5/4}}{(1-x)^{1/4}}\left(1-\frac{\lambda}{2}\frac{x^{1/2}}{(1-x)^{1/2}}\right)^{1/2}, \tag{9}$$

for a fixed value of the scaled impact parameter $y=\rho/2n_*^2$. Here $x=R/2n_*^2$ is the scaled internuclear separation, and $\lambda=n_*|\Delta E_{n',nl}|/V$ is the inelasticity parameter for the $nl\to n'$ transition. The impact parameter $\rho_{\max}$ in Eq. (6) is the maximum possible value of ρ in the classically allowed region determined by the inelasticity parameter λ of the $nl\to n'$ transition and by the principal quantum number n_*. Within the framework of the semiclassical approach, the transition probability $W_{n',nl}(\rho)$ becomes zero for $\rho>\rho_{\max}(\lambda)$. It corresponds to the maximum value of $\phi_\lambda(x)$. The impact parameter $\tilde{\rho}=2n_*^2\tilde{y}$ in Eq. (6b) is determined by the relation $\tilde{y}=\phi_\lambda(\tilde{x})=\tilde{x}$, where $\tilde{x}=\tilde{R}/2n_*^2$. From Eq. (9) we obtain

$$\tilde{\rho}(\lambda)=2n_*^2\tilde{y}(\lambda),\quad \tilde{y}(\lambda)=1/(1+\lambda^2), \tag{10a}$$

$$\rho_{\max}(\lambda)=2n_*^2\phi_\lambda^{\max},\quad y_{\max}(\lambda)=\phi_\lambda^{\max}. \tag{10b}$$

Thus $\tilde{\rho}$ and $\rho_{\max}$ are determined only by the inelasticity parameter λ and by the principal quantum number n, whereas $\tilde{\rho}<\rho_{\max}$ for given n_* and λ.

Parameter ρ_0 can be calculated from Eq. (2) using expression (6) for the transition probability. It is determined by the principal quantum number n_* and the energy defect $|\Delta E_{fi}|$, as well as by the particular type of colliding partners and their relative velocity V. It should be noted that the roots $x_1^{(\lambda)}(y)$ and $x_2^{(\lambda)}(y)$ of Eq. (9) depend significantly on λ. In the particular case of a pure elastic transition ($|\Delta E_{n',nl}|=0$ and hence $\lambda=0$), when $\tilde{y}=1$ and $y_{\max}=1$, we have $x_{1,2}^{(\lambda)}(y)=1$. The basic expression for the transition probability can be written as

$$W_{n',nl}(\rho,V)=\begin{cases} c, & 0<\rho<\rho_0\\ \dfrac{L_{\text{eff}}^2}{\pi n_*^6V^2\sqrt{\rho}}\mathcal{K}[k(\rho)], & \rho_0<\rho<2n^2\\ 0, & 2n^2<\rho<\infty,\end{cases} \tag{11}$$

where $\mathcal{K}(k)$ is the complete elliptic integral of the first kind [24]

$$\mathcal{K}(k)=\int_0^{\pi/2}(1-k^2\sin^2\theta)^{-1/2}d\theta,$$

$$k(\rho)=\sqrt{(1-\rho/2n^2)/2}. \tag{12}$$

Integration of Eq. (6) over all impact parameters leads to the following result for the cross section of the inelastic $nl\to n'$ transition [9]:

$$\sigma_{n',nl}=\begin{cases} c\pi\rho_{\max}^2(\lambda), & \rho_0>\rho_{\max}\\ c\pi\rho_0^2+\dfrac{2\pi L_{\text{eff}}^2}{V^2n_*^3}\mathcal{F}_\lambda(\rho_0/2n_*^2), & \rho_0\leqslant\rho_{\max},\end{cases} \tag{13a}$$

where the function $\mathcal{F}_\lambda(y_0)$ can be written as

$$\mathcal{F}_*(y_0)=\frac{1}{\pi}\left\{2\Theta(\tilde{y}-y_0)\int_{y_0}^{\xi_1}\left(\frac{x^2-y_0^2}{x-x^2}\right)^{1/2}dx+\int_{\xi_1}^{\xi_2}\left(\frac{x^2-y_0^2}{x-x^2}\right)^{1/2}dx+\mathcal{Q}(\xi_2)-\mathcal{Q}(\xi_1)\right\}, \tag{13b}$$

$$\mathcal{Q}(z)=\arctan\left[\left(\frac{z}{1-z}\right)^{1/2}\right]-[z(1-z)]^{1/2}+\lambda\left[z-\ln\left(\frac{1}{1-z}\right)\right].$$

Here $y_0=\rho_0/2n_*^2$ is determined from the normalization condition (2) for the transition probability $W_{n',nl}^{\text{pt}}(y)$ calculated by the first-order perturbation theory. Parameters $\xi_{1,2}=x_{1,2}^{(\lambda)}(y_0)$ are the roots of Eq. (9) for a given value of the scaled impact parameter $y_0=\rho_0/2n_*^2$, and $\tilde{y}=\tilde{y}(\lambda)$ is given by Eq. (10).

B. The effective scattering length

It is well known that the scattering length approximation $f_{eB}=-L=$ const for the amplitude of elastic scattering of ultralow energy electrons by heavy rare-gas atoms is valid only in the close vicinity to zero energy. Due to the presence of the long-range polarization potential [14,15] the differential cross section $|f_{eB}(k,\theta)|^2$ strongly drops with an increase of the electron momentum. It reaches the deep Ramsauer-Townsend minimum in the range of electron energy $\epsilon=k^2/2\equiv 0.2-1$ eV depending on the scattering angle and the particular type of atom, and then rapidly increases. Recent measurements of the cross sections in the vicinity of the Ramsauer-Townsend minimum can be found in Refs. [25,26].

Previous attempts to include this dependence in the theory of Rydberg-atom collisions [11–13] incorporate the dependence of the effective cross section on n. We suggest here a method which includes also dependence on the inelasticity parameter. Note first that in the strong-coupling region the transition probabilities do not depend significantly on the specific form of the electron-perturber interaction. It can be seen directly from Eq. (13) at $\rho_0\to\rho_{\max}$ and reflects a general feature of any collisional processes involving a large number of closely spaced levels. Indeed for strong collisions the quenching cross section for a given energy level is practically the same as the total scattering cross section, which is determined by the unitarity condition.

Thus the required modification of the scattering amplitude can be accomplished in the weak-coupling limit. We will do it within the framework of the quasi-free-electron model. We proceed from the general semiclassical formula for the cross section of the $nl\to n'$ transition in the momentum representation [27].

$$\sigma_{n',nl}=\frac{\pi}{2^{1/2}V^2(n')^3}\int_{k_{\rm min}}^{\infty}k^2dk|g_{nl}(k)|^2\times\int_{-1}^{\nu_{\rm max}(k)}\frac{d(\cos\theta)}{(1-\cos\theta)^{1/2}}|f_{eB}(k,\theta)|^2. \quad (14a)$$

Here $f_{eB}(k,\theta)$ is the exact amplitude for elastic scattering of a free electron by the atom B; k and θ are the momentum and scattering angle; $\nu_{\rm max}(k)$ and $k_{\rm min}$ are given by

$$\nu_{\rm max}(k)=1-2k_{\rm min}^2/k^2,\quad k_{\rm min}=Q_{\rm min}/2\approx|\Delta E_{n',nl}|/2V, \quad (14b)$$

$|g_{nl}(k)|^2$ is the momentum distribution function of the Rydberg electron in the initial nl state. For the nl states with low orbital angular momentum ($l\gg n$) we will use the semiclassical result [28].

$$|g_{nl}(k)|^2=\frac{4n_*}{\pi}\frac{1}{k^2(1+n_*^2k^2)^2},\quad l\ll n, \quad (15)$$

corresponding to the pure classical momentum distribution function of the electron in the Coulomb field of the ion core [3]. In the scattering length approximation ($f_{eB}=-L$ =const) the general formula (14) yields the following analytical result

$$\sigma_{n',nl}^L(\lambda)=\frac{2\pi L^2}{V^2(n')^3}f_{n',nl}(\lambda), \quad (16a)$$

$$f_{n',nl}(\lambda)=\frac{2}{\pi}\left[\arctan\left(\frac{2}{\lambda}\right)-\frac{\lambda}{2}\ln\left(1+\frac{4}{\lambda^2}\right)\right],$$

$$\lambda=n_*|\Delta E_{n'nl}|/V. \quad (16b)$$

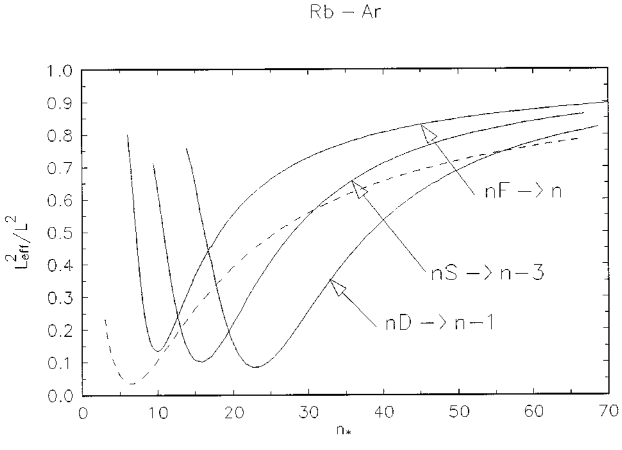

FIG. 1. n dependence of the ratio $L_{\rm eff}^2/L^2$ for the e-Ar scattering. Full curves are the present results, Eq. (17) for the $nS\rightarrow n-3$, $nD\rightarrow n-1$, and $nF\rightarrow n$ transitions in the Rb (nl)+Ar collisions at E=0.026 eV. Dashed curve presents the ratio $\sigma_{\rm el}(\epsilon_n)/4\pi L^2$, where $\epsilon_n=1/2n_*^2$ is the mean kinetic energy of the orbital electron motion.

Expression (16) was derived simultaneously in Ref. [29] by the semiclassical impact-parameter method in the first-order perturbation theory and in Ref. [30] using the impulse approximation and binary-encounter theory for the atomic form factors [31,32]. It should be noted that for pure quasielastic $nl\rightarrow n'$ transition without energy transfer ($\lambda=0$) expression (16) yields $f_{n',nl}(\lambda=0)=1$. Hence Eq. (16) includes the well-known Omont's [33] result $\sigma_{n',nl}=2\pi L^2/V^2n^3$ as a particular case.

Comparison of Eq. (16) with the general formula (14) allows us to introduce a parameter $L_{\rm eff}^2(n_*,\lambda)$ which we use to calculate cross sections according to Eqs. (6) and (13). The ratio $L_{\rm eff}^2/L^2$ can be also written as $\sigma_{n',nl}/\sigma_{n',nl}^L$ where $\sigma_{n',nl}$ is calculated in the impulse approximation (14) with actual scattering amplitude $f_{eB}(k,\theta)$, while $\sigma_{n',nl}^L$ is the corresponding value obtained for $f_{eB}=-L=$const Eq. (16). It is convenient to rewrite $L_{\rm eff}^2(n_*,\lambda)$ as

$$L_{\rm eff}^2(n_*,\lambda)=\frac{2^{1/2}}{\pi f_{n',nl}(\lambda)}\int_{z_{\rm min}}^{\infty}\frac{dz}{(1+z^2)^2}\times\int_{-1}^{\nu_{\rm max}(z)}\frac{d(\cos\theta)}{(1-\cos\theta)^{1/2}}|f_{eB}(k=z/n_*,\theta)|^2, \quad (17)$$

where

$$\nu_{\rm max}(z)=1-2z_{\rm min}^2/z^2,\quad z_{\rm min}=n_*|\Delta E_{n',nl}|/2V=\lambda/2. \quad (18)$$

In the scattering length approximation $f_{eB}=-L$, formula (17) yields $L_{\rm eff}(n_*,\lambda)\equiv L=$const . In a general case it incorporates both the short- and long-range parts of the electron-perturber interaction. The parameter $L_{\rm eff}(n_*\lambda)$ characterizes the actual electron-atom interaction in the range of the electron momenta which gives the main contribution to the $nl\rightarrow n'$ transition for given n, relative velocity V, and energy defect $|\Delta E_{n',nl}|$. Therefore $L_{\rm eff}(n_*,\lambda)$ depends both on n and the inelasticity parameter $\lambda=n_*|\Delta E_{n',nl}|/V$.

For calculation of the scattering amplitude we use the partial-wave expansion in terms of the scattering phase shifts η_l, where l is the electron angular momentum *relative to the perturber*. Within the framework of the modified effective range theory [14,15], η_l at low energies may be calculated using the analytical expressions

$$k^{-1}\tan\eta_0=-L-\frac{\pi\alpha}{3}k-\frac{4\alpha L}{3}k^2\ln k+D_0k^2+F_0k^3+O(k^4), \quad (19a)$$

$$k^{-1}\tan\eta_1=\frac{\pi\alpha k}{15}-D_1k^2+O(k^3), \quad (19b)$$

$$k^{-1}\tan\eta_l=\frac{\pi\alpha k}{(2l+3)(2l+1)(2l-1)}+O(k^3),\quad l\geq 2. \quad (19c)$$

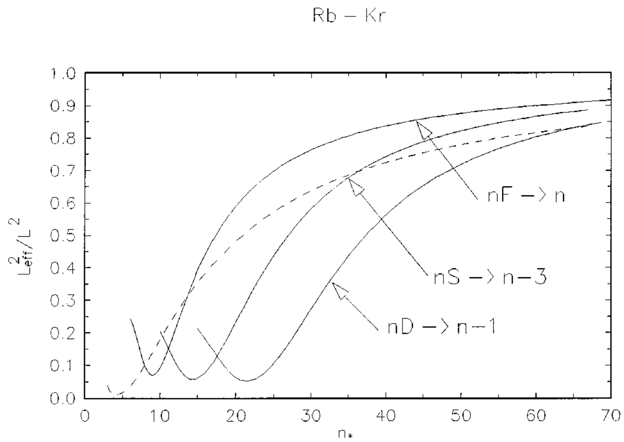

FIG. 2. The same calculations as in Fig. 1 for the Rb(nl)+Kr $\rightarrow$Rb(n')+Kr transitions.

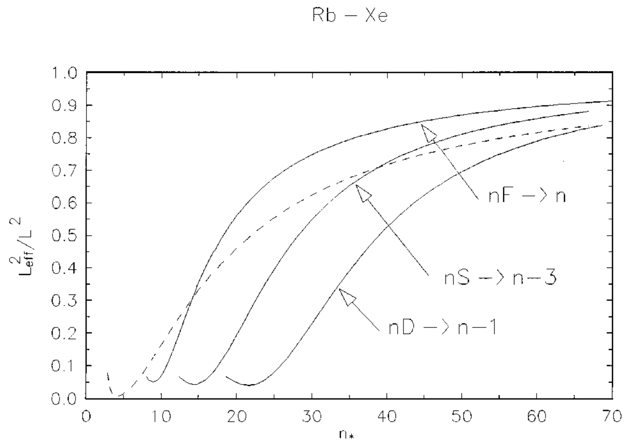

FIG. 3. The same calculations as in Fig. 1 for the Rb(nl)+Xe $\rightarrow$Rb(n')+Xe transitions.

Here α is the polarizability of the perturbing atom, and D_0, D_1, and F_0 are the constant coefficients. In the present calculations we used experimentally obtained values [26]. Note that the case of atoms with high polarizabilities (e.g., alkali-metal atoms) needs a special analysis [34].

The present calculations of the effective scattering length were performed for transitions to the nearest energy levels which provide the major contribution to the quasielastic or inelastic transitions. For the relative velocities of colliding atoms we took $V=(2T/\mu)^{1/2}$, where T is the gas temperature. The results for the ratio L^2_{eff}/L^2 are plotted in Figs. 1, 2, and 3. The ratio L^2_{eff}/L^2 depends significantly on n and turns out to be quite different for transitions with small and large energy defects. In all cases the deep minimum in L^2_{eff}/L^2 results from the Ramsauer-Townsend effect in free-electron scattering, but it occurs at different values of n_* ($n_*=10$, 15, and 23 for $nF\rightarrow n$, $nS\rightarrow n-3$, and $nD\rightarrow n-1$ transitions, respectively). Simple estimates of the typical electron momentum $k\sim k_{\text{min}}=|\Delta E_{n',nl}|/2V$ at $n_*\approx 10$, 15, and 23 show that they are in full agreement with the values of the free-electron momentum which corresponds to the Ramsauer-Townsend minimum. Note also that the use of $[\sigma_{\text{el}}(\epsilon_n)/4\pi]^{1/2}$ [11,12], instead of the standard scattering length L, improves the results. However, more accurate calculations should incorporate the dependence of L_{eff} on the energy defect.

Thus we confirm the previous conclusions [12,13] that the standard scattering length approximation $f_{eB}=-L=\text{const}$ becomes inapplicable for collisions of Rydberg atoms with the heavy rare-gas atoms, in contrast to the case of the helium atom as a perturber. For reliable quantitative results on inelastic and quasielastic transitions induced by collisions with Ar, Kr, and Xe we need an appropriate description of both the short- and long-range parts of the electron-perturber interaction.

C. Analysis of probabilities and cross sections as functions of the inelasticity parameter and the collision strength parameter

Analysis of the basic Eqs. (6), (13) in a particular case of pure quasielastic $nl\rightarrow n'$ transitions ($n'=n$) with a change in the orbital angular momentum alone without energy transferred to the Rydberg atom ($\Delta E_{n,nl}=0$, or $\lambda=0$) was performed in Ref. [9]. In the present work we analyze the general case of inelastic $nl\rightarrow n'$ transitions with the change of both the orbital and principal quantum numbers for an arbitrary magnitude of the inelasticity parameter $\lambda=n_*|\Delta E_{n',nl}|/V$.

1. Transition probabilities

For further analysis it is convenient to rewrite Eqs. (6) and (13) in terms of scaled parameters $x=R/2n_*^2$ and $y=\rho/2n_*^2$. Note that the radius $r_n=2n_*^2$ corresponds to the right turning point in the Coulomb potential $r_2\approx n_*^2(1+e)$ at $l\ll n_*$, when the eccentricity of the orbit $e\approx 1$ [see Eq. (5)]. For the transition probability we obtain

$$W_{\zeta,\lambda}(y)=\begin{cases} c, & 0\leqslant y\leqslant y_0 \\ \dfrac{\zeta}{\pi\sqrt{2}}\left(2\Theta(\tilde{y}-y)\displaystyle\int_y^{x_1(y)}\frac{dx}{\sqrt{(x-x^2)(x^2-y^2)}}+\int_{x_1(y)}^{x_2(y)}\frac{dx}{\sqrt{(x-x^2)(x^2-y^2)}}\right), & y_0\leqslant y\leqslant y_{\max} \\ 0, & y_{\max}\leqslant y \end{cases} \tag{20}$$

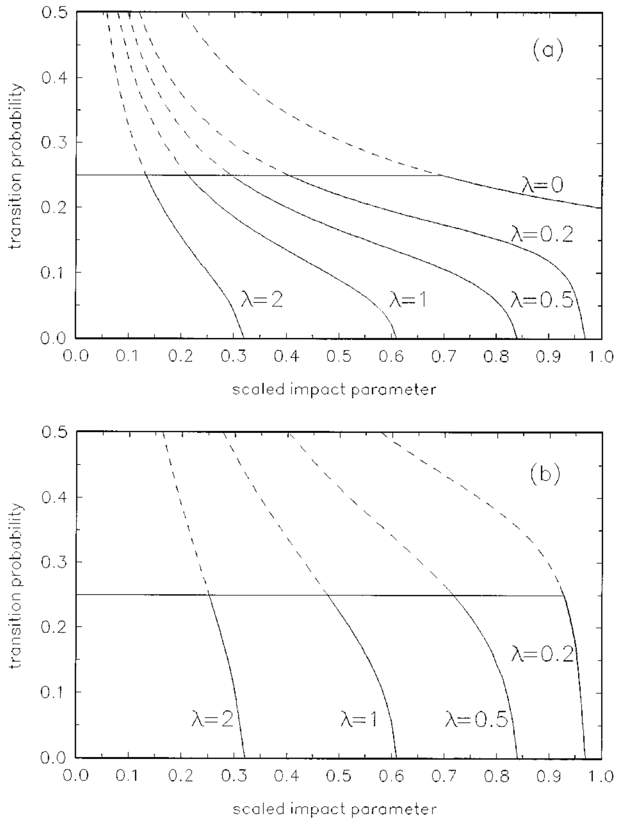

FIG. 4. Transition probability $W_{\zeta,\lambda}(y)$, Eq. (20) as a function of the scaled impact parameter $y=\rho/2n_*^2$ for different inelasticity parameters $\lambda=n_*|\Delta E_{n',nl}|/V$ ($\lambda=0$; 0.2 and 0.5). Figures 1(a) and 1(b) correspond to $\zeta=0.2$ and 0.5 of the collision strength $\zeta=L_{\rm eff}^2/2^{3/2}V^2n_*^7$, respectively.

where $\zeta=L_{\rm eff}^2/2^{3/2}V^2n_*^7$ is a scaled parameter characterizing the collision strength. The results of the present calculations for the transition probability as a function of the scaled impact parameter $y=\rho/2n_*^2$ are presented in Figs. 4(a) and 4(b) for different values of the inelasticity parameter ($\lambda=0$, 0.2, 0.5, 1, and 2) and the collision strength ($\zeta=0.2$ and 0.5). In the region $0\leqslant\rho\leqslant\rho_0$ the first-order probability $W_{\lambda\zeta}^{\rm pt}(\rho)$ becomes large and should be normalized to a constant c according to the normalized perturbation theory. Figure 4 demonstrates how the chosen value $c=0.25$ limits the growth of $W^{\rm pt}$.

The probability $W_{\lambda\zeta}^{\rm pt}(\rho)$ becomes zero at $\rho>\rho_{\rm max}$. This happens because the semiclassical approach neglects the exponentially decaying tail of the electron wave function. The maximum impact parameter $\rho_{\rm max}$ depends substantially on the inelasticity parameter λ. To analyze this dependence, we will proceed from the conservation of energy law for collisional $nl\rightarrow n'$ transition

$$E_{nl}+q^2/2\mu=E_{n'}+(q')^2/2\mu,\quad E_{nl}=-1/2(n-\delta_l)^2,$$

$$E_{n'}=-1/2(n')^2, \tag{21}$$

where $q^2/2\mu$ and $(q')^2/2\mu$ are the kinetic energies of colliding atoms in the initial and final states, respectively. According to Eq. (21), the minimum possible value of the momentum transfer $Q=|\mathbf{q}'-\mathbf{q}|$ is determined by the relation $Q_{\rm min}\approx|\Delta E_{n',nl}|/V$ if the kinetic energy $q^2/2\mu$ of colliding atoms is considerably greater than the energy defect $|\Delta E_{n',nl}|$ of the $nl\rightarrow n'$ transition. The minimum value of the Rydberg electron momentum k for the $nl\rightarrow n'$ transition with the energy transfer $|\Delta E_{n',nl}|$ is $k_{\rm min}\approx|\Delta E_{n',nl}|/2V$. It corresponds to the backward scattering ($\mathbf{k}'=-\mathbf{k}$) of the Rydberg quasifree electron by the perturber B. Substitution of $k_{\rm min}=\lambda/2n_*$ into the classical expression

$$k^2/2-1/r=-1/2n_*^2 \tag{22}$$

for the energy of the Rydberg electron in the Coulomb field of the ion core A^+, yields

$$r_{\rm max}(\lambda)=\frac{2n_*^2}{1+(n_*k_{\rm min})^2}=\frac{2n_*^2}{1+(\lambda/2)^2}. \tag{23}$$

Within the framework of the Fermi pseudopotential model for the electron-perturber interaction, the collisional transition of the Rydberg electron occurs when its radius r relative to the ion core A^+ is equal to separation R between A^+ and B. Thus Eq. (23) for the radius $r_{\rm max}(\lambda)$ corresponds to the maximum possible value of the internuclear separation, and therefore can be considered as an upper bound for $\rho_{\rm max}$.

As is seen from Fig. 4, for each λ there is a certain impact parameter ρ_0 which separates the regions of weak and strong coupling. The dependence $\rho_0(\lambda)$ is demonstrated in Fig. 5 for different values of the collision strength ζ (full curves). For comparison we also present $\rho_{\rm max}(\lambda)/2n_*^2$. At large $\zeta>1$

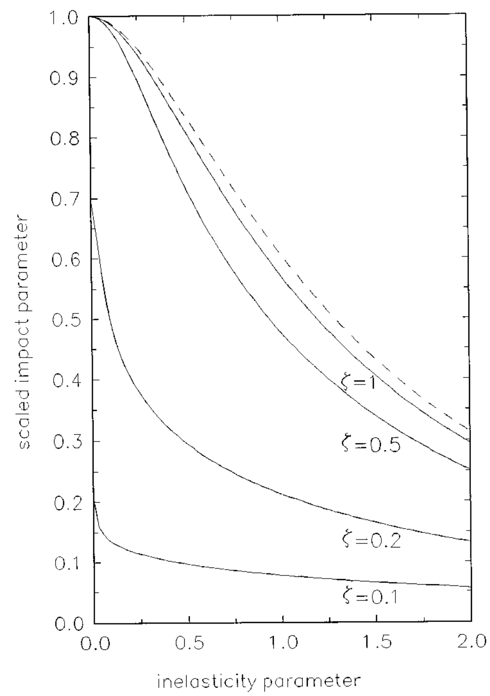

FIG. 5. Scaled impact parameter $y_0=\rho_0/2n_*^2$, separating the close- and weak-coupling regions, as a function of the inelasticity parameter λ for different collision strengths $\zeta=0.1$, 0.2, 0.5, and 1 (full curves). Dashed curve represents the maximum possible scaled impact parameter $\rho_{\rm max}(\lambda)/2n_*^2$.

practically the whole range of classically allowed impact parameters $0<\rho<\rho_{\max}(\lambda)$ corresponds to the strong coupling of Rydberg states. The first-order perturbation theory becomes inapplicable for almost all possible values of $y=\rho/2n_*^2$.

2. Cross sections

Equation (13a) for the cross section of the inelastic $nl\rightarrow n'$ transition can be rewritten in terms of the scaled parameters λ and ζ

$$\sigma(\lambda,\zeta)=\pi n_*^4\times\begin{cases}4cy_{\max}^2(\lambda), & y_0=y_{\max}\\ 4cy_0^2(\lambda,\zeta)+2^{5/2}\zeta\mathcal{F}_\lambda(y_0), & y_0\leqslant y_{\max}\end{cases}\tag{24}$$

Here $y_{\max}=\rho_{\max}(\lambda)/2n_*^2$; $y_0=\rho_0(\lambda,\zeta)/2n_*^2$ should be calculated from equation $W_{\lambda\zeta}(y_0)=c$ in which the first-order transition probability is given by Eq. (20); and the $\mathcal{F}$ function is determined by Eq. (13b). Note that $\mathcal{F}_\lambda(y_0)\rightarrow 0$ when $y_0(\lambda,\zeta)\rightarrow y_{\max}(\lambda)$, i.e., for large collision strength ζ. The ratio of the cross section $\sigma_{n',nl}$ to the geometric area of the Rydberg atom depends only on λ and ζ. Thus it is interesting to analyze the scaled cross section $\sigma_{n',nl}/\pi n_*^4$ as a function of the inelasticity parameter λ and the collision strength ζ.

According to Eq. (24) the drop of the total cross section $\sigma_{n',nl}=\Sigma_{l'}\sigma_{n'l',nl}$ of the $nl\rightarrow n'$ transition with increasing energy defect is actually determined by the parameter λ. This fact was first established by several authors [18,29,30] who independently obtained analytical expressions for the cross sections of inelastic transitions in the region of weak coupling. This parameter is more relevant to the cross sections summed over all final l' sublevels whereas the reduced parameter $\gamma=n^2|\Delta E_{n',nl}|/V$ was used by Hickman [11] in the empirical scaling formula for the l-mixing collisions. At the same time the parameter $\beta^2=(L_{\text{eff}}/Vn^{3.337})^2$ of Hickman's formula is very close to the parameter $\zeta=L_{\text{eff}}^2/2^{3/2}V^2n_*^7$ characterizing the efficiency of collision within the framework of semiclassical approach [9].

The scaling formula (24) has a simple analytical form in two limiting cases. The first corresponds to pure quasielastic transitions without energy transfer ($\lambda=0$) to the Rydberg atom. In this case $y_{\max}=1$, and from Eq. (24) we obtain

$$\sigma_{\lambda=0}(\zeta)=\pi n_*^4\times\begin{cases}4c, & y_0=1\\ 4cy_0^2(\zeta)+\dfrac{2^{7/2}\zeta}{\pi}\displaystyle\int_{y_0}^{1}\left(\frac{x^2-y_0^2}{x-x^2}\right)^{1/2}dx, & y_0<1.\end{cases}\tag{25}$$

$y_0(\zeta)$ is determined from the equation $(2\zeta/\pi y_0^{1/2})\mathcal{K}[k(y_0)]=c$. Hence, it is approximately equal to $(\zeta/c)^2$ since $\mathcal{K}(k)\approx\pi/2$ for $0\leqslant k\leqslant 2^{-1/2}$, when $0\leqslant y\leqslant 1$. For $\lambda=0$ there is a certain boundary value of the collision strength $\zeta_0=c$ (and hence the principal quantum number $n_*=n_0$) for which the scaled parameter y_0 reaches $y_{\max}$. This results from the nonzero value of the transition probability at $y_{\max}(\lambda=0)=1$, in contrast to the general case of $\lambda\neq 0$ when $W[(y_{\max}(\lambda)]=0$ (see Fig. 4). The strong-coupling region corresponds to $\zeta\geqslant c$.

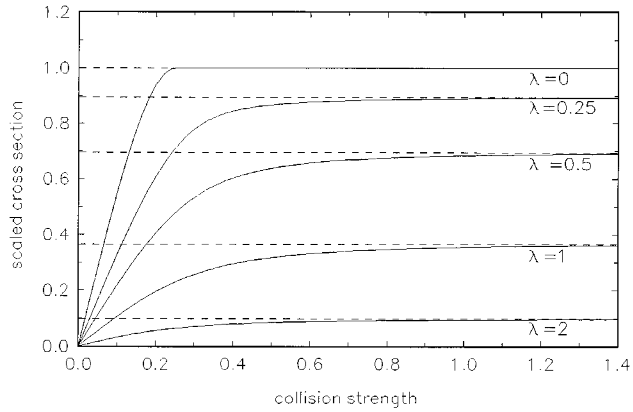

FIG. 6. The ratio $\sigma_\lambda(\zeta)/\pi n_*^4$ of the cross section to the geometric area of the Rydberg atom as a function of the collision strength ζ. Full curves were calculated by Eqs. (25) and (13b). Dashed curves represent the limiting value of this ratio at $\zeta\rightarrow\infty$ for $\lambda\neq 0$ and $\zeta\geqslant\zeta_0\approx c$ for $\lambda=0$ [see Eqs. (25) and (26)]. Numbers near the curves mark the values of the inelasticity parameter λ.

In the weak-coupling region $\zeta\ll c$ ($n_*\gg n_0$) the total cross section, Eq. (26) approaches the asymptotic expression $\sigma_{n,nl}=2^{5/2}\zeta\pi n_*^4$. This limiting expression is in full agreement with Omont's result [33]. In this case the magnitude of the quasielastic cross section is much lower than the geometric area of Rydberg atom.

The second case corresponds to inelastic $nl\rightarrow n'$ transitions in the range of weak coupling $\zeta\ll 1$. The contribution of the strong-coupling region $0\leqslant\rho\leqslant\rho_0$ can be neglected. Thus assuming $y_0=\rho_0/2n_*^2\rightarrow 0$ in Eqs. (13b) and (24), we have $\mathcal{F}_{y_0=0}(\lambda)\rightarrow f_{n',nl}(\lambda)$, where f is defined by Eq. (16b). For the scaled cross section we obtain

$$\sigma_{n',nl}(\lambda,\zeta)=2^{5/2}\zeta\pi n_*^4 f_{n',nl}(\lambda).\tag{26}$$

This expression is in full agreement with analytical result (16) of the first-order perturbation theory derived in Refs. [29,30]. For pure quasielastic transitions the $f_{n',nl}(\lambda)$ function in Eq. (26) becomes equal to one, while the collision strength parameter $\zeta_0\approx c$. Hence, the aforementioned Omont's formula [33] for the l-mixing cross section in the range of weak coupling may be derived simultaneously both from Eqs. (25) and (26).

The general case, given by Eq. (24), is presented in Figs. 6 and 7. Figure 6 demonstrates the scaled cross section $\sigma_\lambda(\zeta)/\pi n_*^4$ as a function of ζ for different values of λ. Note that the inelastic cross section strongly falls with increasing inelasticity parameter λ both in the range of weak and strong coupling.

To demonstrate the failure of the perturbative approach in the strong-coupling region, we make a comparison between the present calculations and the first-order perturbation theory in Fig. 7. The results are presented for $\zeta=0.1$, 0.25, and 1. For each couple of curves, the lower one has been calculated using the scaling formula (24), while the upper curves have been obtained in the first-order perturbation

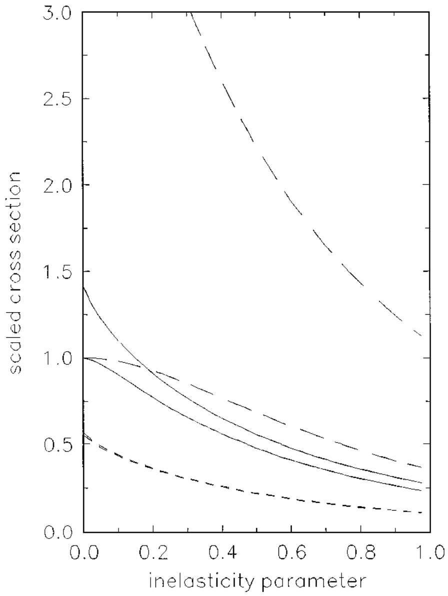

FIG. 7. The scaled cross section $\sigma_\zeta(\lambda)/\pi n_*^4$ as a function of the inelasticity parameter λ. Short-dashed, full, and long-dashed couples of curves are the present semiclassical calculations for $\zeta=0.1$, 0.25, and 1, respectively. The lower curves for each couple were calculated using the scaling formula (24), while the upper curves correspond to the first-order perturbation theory, Eqs. (26) and (16b).

theory. The first-order perturbation theory gives satisfactory results at $\zeta<0.1$. In this case the cross sections are very close to those calculated by the normalized perturbation theory. Note that the difference between these two methods becomes particularly small for large λ. However, at intermediate ζ (full curves for $\zeta=0.25$) both methods give close results only for inelastic transitions with large λ. The difference becomes very large at small λ and large $\zeta>1$. In this strong-coupling case the first-order perturbation theory (or impulse approximation in the momentum representation) leads to significantly overestimated magnitudes and to qualitatively incorrect behavior of the cross section (see long-dashed curves for $\zeta=2$).

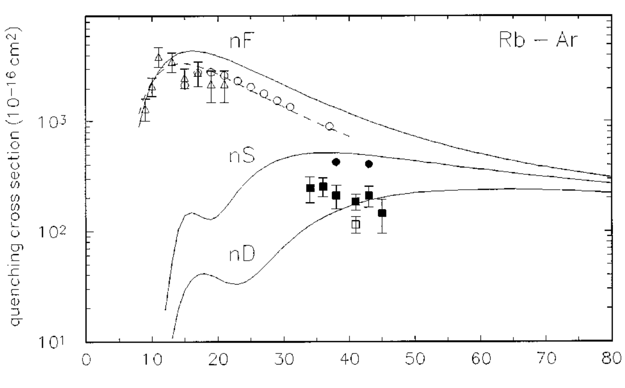

FIG. 8. Cross sections for quenching of the nS-, nD-, and nF-states of the Rydberg Rb atom by Ar averaged over the Maxwellian velocity distribution. Full curves, the present results calculated by Eq. (13) ($T=296$ K). Dashed curve, the same calculation for the nF level at $T=520$ K. Full squares, empty squares, and triangles are the experimental data for the nS-, nD levels (Ref. [36], $T=296$ K), and nF levels (Ref. [35], $T=520$ K), respectively. Full circles and empty circles are the free-electron-model calculations [16,17] for nS and nF states, respectively.

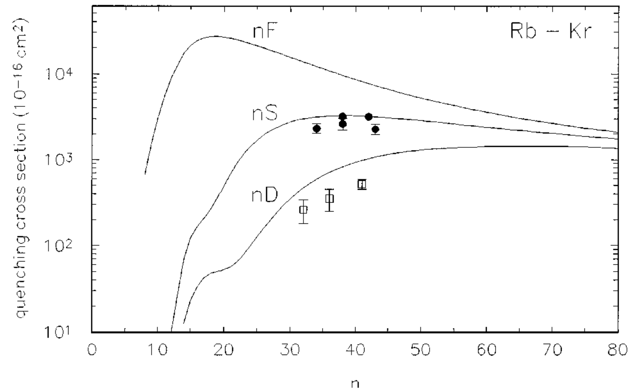

FIG. 9. The same as in Fig. 8 for quenching by Kr atoms. Full circles, theory of Sato and Matsuzawa [17] for nS states.

III. RESULTS AND DISCUSSION: COMPARISON WITH EXPERIMENT

In this section we apply our theory to calculations of the quenching cross sections for the Rydberg nS, nD, and nF states of the rubidium atom in thermal collisions with Ar, Kr, and Xe. The experimental data are available both for nF level [35] having a small quantum defect ($\delta_f=0.02$), and for isolated nS, nD levels [36] (for which $\delta_s=3.13$, $\delta_d=1.34$). Note that the present calculations are by no means exhaustive with regard to comparison with existent experimental data. Rather, they illustrate the results of our approach in a wide range of n and reaction energy defects.

Our cross sections include the summation over all possible values of the final principal quantum number n', i.e., we calculate

$$\sigma_{nl}=\sum_{n'}\sigma_{n',nl}. \tag{27}$$

This summation leads to a slow decrease of the quenching cross section in the high-n limit. For very high $n\gg 1/V^{1/2}$

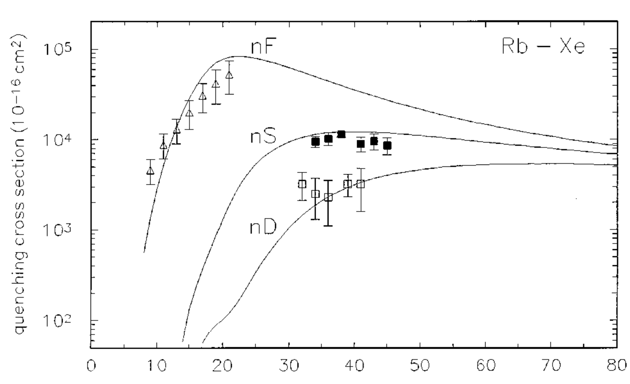

FIG. 10. The same as in Fig. 8 for quenching by Xe atoms.

limit (this region is not shown in the figure) the quenching cross section decays as $1/n$ [3]. The cross section σ_n is averaged then over the Maxwellian distribution of relative velocities according to $\langle\sigma_{nl}\rangle=\langle V\sigma_{nl}(V)\rangle/\langle V\rangle_T$, where $\langle V\rangle_T=(8T/\pi\mu)^{1/2}$ is the mean velocity for a given gas temperature T, and μ is the reduced mass.

The n dependencies of the averaged quenching cross sections for nS, nD, and nF states of Rb atoms in thermal collisions with Ar, Kr, and Xe are shown in Figs. 8–10. They are compared with experimental data of Refs. [35,36]. For the quenching of the nF and nS levels by Ar and nF levels by Kr we also show previous theoretical data of Refs. [16,17] obtained in the impulse approximation. Overall, our calculations reproduce the experimental observations of Hugon *et al.* [35,36] quite well, although there is a substantial disagreement (about a factor of two) for the quenching of nS states by Ar. Sato and Matsuzawa's results [17] are slightly lower than ours in this region of n, but they also substantially exceed the experimental data.

The quenching cross sections reveal strong dependence on the quantum defect δ_l of the initial Rydberg nl state in the whole experimentally studied range of n. This behavior is reasonably reproduced by our semiclassical calculations for quasielastic l-mixing quenching of nF levels as well as for inelastic n,l-changing quenching of nS and nD levels. Note that the impulse approximation does not describe the observed cross sections for the quenching of nF states in the range $n<25-30$, where it is mainly determined by the quasielastic l-mixing collisions. On the other hand, for $n>40$–50 the cross sections, corresponding to different values of the initial orbital angular momentum, start to merge. This occurs due to contribution of a large number of different $nl\rightarrow n'$ transitions ($\Delta n=0,\pm1,\pm2,\ldots$) which makes the total quenching cross section independent of quantum defect in accordance with the well-known results of the asymptotic theory [33].

Another interesting feature of the results is nonmonotonic dependence of the calculated cross sections for nS and nD levels on n in the region of n from 15 to 25. This feature is a manifestation of the Ramsauer-Townsend effect which is clearly represented in the n dependence of the effective scattering length Figs. 8–10. Although averaging over the Maxwellian distribution in relative velocities makes this influence somewhat less pronounced than that for a fixed relative velocity, the Ramsauer–Townsend minimum affects significantly the quenching process in Rb—Ar collisions at $n=15$–30. Unfortunately there is no experimental data available in this region. For the process of quenching by the Kr atoms the Ramsauer-Townsend minimum is less pronounced since it occurs at higher energies in the free-electron scattering. The Maxwell average washes out this effect completely for Xe. In order to demonstrate the Ramsauer–Townsend effect for a fixed collision velocity, we present in Fig. 11 the nonaveraged cross sections for quenching of Rb(nD) states. Now the effect becomes visible even for Xe but, as before, it is best pronounced for Ar.

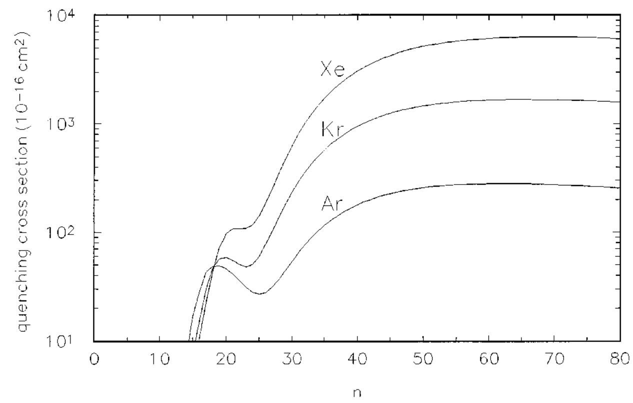

FIG. 11. Nonaveraged cross sections for quenching of nD states by Ar, Kr, and Xe. The collision velocity equals the mean velocity at temperature 296 K for each Rb—B pair.

IV. CONCLUSION

In summary, we have obtained simple scaling formulas for the probabilities and cross sections of $nl\rightarrow n'$ transitions in Rydberg-atom–neutral-particle collisions, using semiclassical expressions [9] of the normalized perturbation theory. These formulas contain only two physical parameters, λ and ζ. Inelasticity parameter λ describes the transition energy defect. The efficiency of the transition is determined by the collision strength parameter ζ. Analysis of the probability $W_{\lambda\zeta}(\rho/2n_*^2)$ and scaled cross section $\sigma_{\zeta\lambda}/\pi n_*^4$ behavior has been done in a wide range of ζ and λ. The obtained data for the cross sections describe a wide region of the principal quantum number n, the relative velocity V, and the energy defect $|\Delta E_{n',nl}|$. Thus a reasonable description of quasielastic l-mixing and inelastic n,l-changing processes was simultaneously given from a common point of view independently of a particular value of the energy transferred to the Rydberg atom.

In the simplest case of the scattering length approximation, the well-known asymptotic formula [33] fo pure quasielastic l-mixing collisions follows directly from Eq. (24) in the range of weak coupling $\zeta\ll1$. Moreover, general analytical formula (16) [see also Eq. (26)] for the cross section of inelastic transitions obtained in Refs. [29,30] corresponds to the weak-coupling limit of the normalized perturbation theory. We have also rewritten the limiting analytical expression of Ref. [9] for quasielastic l-mixing collisions in terms of the collision strength parameter ζ. It was shown that the strong-coupling region corresponds to large values of ζ, while in the weak-coupling region the cross section (25) approaches Omont's result.

We have confirmed the previous conclusions [12,13] about the invalidity of the scattering length approximation in the case of the Rydberg-atom–heavy-rare-gas-atom collisions, in contrast to the case of the He atom as a perturber. We have shown how to incorporate the energy and angular dependencies of the free-electron scattering amplitude in a more general way, valid for both quasielastic and inelastic processes. The method is based on the impulse approximation and modified effective range theory. The strong dependence of the electron–heavy-rare-gas-atom scattering amplitude on the momentum and scattering angle affects significantly the values of the cross sections for quasielastic and inelastic transitions. In particular, the electron momenta in the vicinity of the Ramsauer-Townsend minimum contribute significantly to the cross sections of the inelastic processes.

Calculations of the quenching cross sections for the Rydberg nS, nD, and nF states of alkali-metal Rb atom by the ground-state Ar, Kr, and Xe atoms have been carried out in a wide range of the principal quantum numbers. The contribution of a large number of the $nl \rightarrow n'$ transitions from the initial selectively excited nl level to the degenerate manifold of final n' levels were taken into account. The results of present calculations are in reasonable quantitative agreement with experimental data on quenching of Rb atoms for quite different quantum defects of the Rydberg states. Thus the semiclassical approach based on the normalized perturbation theory provides a successful quantitative description of major phenomena in inelastic and quasielastic collisions induced by interaction of Rydberg electron with the rare-gas atoms.

ACKNOWLEDGMENTS

This work has been supported by the National Science Foundation through Grant No. PHY-9509265. V.S.L. acknowledges also financial support from the INTAS Association (1010-CT93-0027), International Science Technological Center (Grant No. 076) and Russian Fund of Fundamental Investigations (Grant 94-02-05371-a).

[1] *Rydberg States of Atoms and Molecules*, edited by R.F. Stebbings and F.B. Dunning (Cambridge University Press, Cambridge, 1983). The theory of Rydberg-atom–neutral-particle collisions is reviewed in the articles: (a) A.P. Hickman, R.E. Olson, and J. Pascale, Ch. 6, p. 187; (b) M. Matsuzawa, Ch. 8, p. 267; (c) M.R. Flannery, Ch.11, p. 393.
[2] T.F. Gallagher, *Rydberg Atoms* (Cambridge University Press, Cambridge, 1994).
[3] I.L. Beigman, and V.S. Lebedev, Phys. Rep. **250**, 95 (1995).
[4] A. Kumar, N.F. Lane, and M. Kimura, Phys. Rev. A **39**, 1020 (1989).
[5] M. Kimura and N.F. Lane, Phys. Rev. A **42**, 1258 (1990).
[6] C.E. Burkhardt and J.J. Leventhal, Phys. Rev. A **43**, 110 (1991).
[7] B. Kaulakys, J. Phys. B **24**, L127 (1991).
[8] H. Liu and B. Li, J. Phys. B **27**, 497 (1994).
[9] V.S. Lebedev (unpublished).
[10] V.S. Lebedev, Zh. Éksp. Teor. Fiz. **103**, 50 (1993) [Sov. Phys. JETP **76**, 27 (1993)].
[11] A.P. Hickman, Phys. Rev. A **23**, 87 (1981).
[12] A.P. Hickman, Phys. Rev. A **19**, 994 (1979).
[13] E. de Prunelé and J. Pascale, J. Phys. B **12**, 2511 (1979).
[14] T.F. O'Malley, L. Spruch, and L. Rosenberg, Phys. Rev. **125**, 1300 (1962).
[15] T.F. O'Malley, Phys. Rev. **130**, 1020 (1963).
[16] K. Sasano and M. Matsuzawa, J. Phys. B **14**, L91 (1981); K. Sasano, Y. Sato, and M. Matsuzawa, Phys. Rev. A **27**, 2421 (1983).
[17] Y. Sato and M. Matsuzawa, Phys. Rev. A **31**, 1366 (1985).
[18] L. Petitjean and F. Gounand, Phys. Rev. A **30**, 2946 (1984).
[19] A.P. Hickman, Phys. Rev. A **18**, 1339 (1978).
[20] M.J. Seaton, Proc. Phys. Soc. **77**, 184 (1961); **79**, 1105 (1962).
[21] I.I. Sobel'man, L.A. Vainshtein, and E.A. Yukov, *Excitation of Atoms and Broadening of Spectral Lines* (Springer, Berlin, 1981).
[22] L.D. Landau and E.M. Lifshitz, *Quantum Mechanics* (Pergamon, Oxford, 1977).
[23] J.I. Gersten, Phys. Rev. A **14**, 1354 (1976).
[24] *Handbook of Mathematical Functions*, edited by M. Abramovitz and I.A. Stegun (Dover, New York, 1965).
[25] J. Ferch, B. Granitza, C. Masche, and W. Raith, J. Phys. B **18**, 967 (1985).
[26] M. Weyhreter, B. Barzick, A. Mann, and F. Linder, Z. Phys. D **7**, 333 (1988).
[27] V.S. Lebedev and V.S. Marchenko, Zh. Éksp. Teor. Fiz. **91**, 428 (1986) [Sov. Phys. JETP 64, 251 (1986)]; J. Phys. B **20**, 6041 (1987).
[28] M. Matsuzawa, J. Phys. B **8**, 2114 (1975); corrigendum: *ibid.* **9**, 2559 (1976).
[29] V.S. Lebedev, and V.S. Marchenko, Zh. Éksp. Teor. Fiz. **88**, 754 (1985) [Sov. Phys. JETP **61**, 443 (1985)].
[30] B. Kaulakys, J. Phys. B **18**, L167 (1985).
[31] M. Matsuzawa, Phys. Rev. A **20**, 860 (1979).
[32] F. Gounand and L. Petitjean, Phys. Rev. A **30**, 61 (1984).
[33] A. Omont, J. Phys. (Paris) **38**, 1343 (1977).
[34] I.I. Fabrikant, J. Phys. B **19**, 1527 (1986); Phys. Rev. A **45**, 6404 (1992).
[35] M. Hugon, F. Gounand, P.R. Fournier, and J. Berlande, J. Phys. B **12**, 2707 (1979).
[36] M. Hugon, B. Sayer, P.R. Fournier, and F. Gounand, J. Phys. B **15**, 2391 (1982).